LETTER

Comparative corrosion behavior of Ni–Mo and Ni–Mo–Cr alloy for applications in reducing environments

H. M. Tawancy

It is well known that a high resistance to reducing environments can be achieved by alloying Ni with Mo. Therefore, Ni–Mo alloys are best suited for applications involving exposure to corrosive environments under reducing conditions, e.g. hydrochloric acid [1]. For example, in the process of crude oil distillation, organic chlorides are decomposed by the entrained water to form HCl, which can lead to excessive corrosion in the condensers, piping systems, and accumulators if they are made of steels. Also, hydrolysis of catalysts in many processes results in HCl.

Experiments show that Mo in Ni-Mo alloys has the effect of increasing anodic polarization and therefore the corrosion rate of the alloy is anodically controlled, e.g. [2, 3]. Although there are a number of Ni–Mo alloys of commercial grade available for applications such as that described above [4], their use can be limited by a series of ordering reactions based upon a DO_{22}-type superlattice, which can degrade the corrosion resistance as well as the mechanical strength [5–7]. In particular, ordering to the D1a superalttice of Ni_4Mo occurs with rapid kinetics at temperatures in the range of 600–800 °C depending upon the exact Mo content leading to property degradation of fabricated components. It is the objective of this paper to demonstrate that this problem could be overcome by critical additions of Cr resulting in deceleration of the ordering kinetics while maintaining properties comparable to those of Cr-free alloys.

Alloys included in the study had nominal chemical compositions of Ni–27Mo, Ni–27Mo–2Cr, Ni–27Mo–3Cr, and Ni–27Mo–4Cr all in weight percent. Table 1 lists the actual compositions. All alloys were processed into sheets 1 mm in thickness. Specimens were solution annealed at 1065 °C and then water quenched. To induce long-range ordering, specimens were aged at temperatures in the range of 500–900 °C and finally air-cooled. Corrosion properties were determined from aqueous corrosion tests in boiling 20% HCl. Corrosion rates were determined from weight loss measurements made on 25.4 mm × 25.4 mm × 1.0 mm specimens after 24-h immersion in HCl and extrapolated to mm/year. Mechanical strength was evaluated from tensile tests (25.4 mm gage length). Light optical metallography, analytical electron microscopy, and Auger electron spectroscopy were used to characterize the microstructure.

All alloys included in the study were found to contain short-range order in the annealed condition as indicated by the presence of diffuse reflections in electron diffraction patterns at {1 1/2 0} positions as reported in earlier studies, e.g. [5]. Figure 1a illustrates the effect of aging time up to 2 h at 500–900 °C

H. M. Tawancy (✉)
Materials Characterization Lab., Center for Engineering Research, Research Institute, King Fahd University of Petroleum and Minerals, P.O. Box 1639, Dhahran 31261, Saudi Arabia
e-mail: tawancy@kfupm.edu.sa

Table 1 Chemical compositions (weight %)

Alloy	Ni	Mo	Cr	Fe	Mn	Si
1	Bal	26.91	>0.1	>0.1	>0.01	>0.05
2	Bal	26.90	1.95	>0.1	>0.01	>0.05
3	Bal	26.95	2.97	>0.1	>0.01	>0.05
4	Bal	26.93	3.94	>0.1	>0.01	>0.05

Fig. 1 Effect of ordering to Ni4Mo in the Ni-27 Mo alloy on its corrosion behavior in boiling 20% HCl. (**a**) Effect of aging time at various temperatures on the corrosion rate. (**b**) Light optical micrograph showing a cross-section of a specimen after corrosion testing (annealed condition). (**c**) Light optical micrograph showing a specimen cross-section after corrosion testing (aged 2 h at 700 °C)
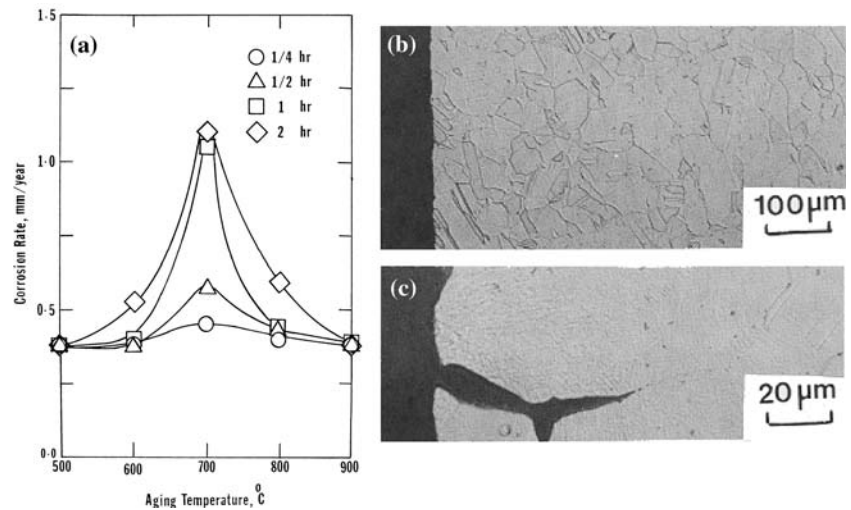
Fig. 2 Effect of ordering to Ni$_4$Mo in the Ni–27Mo alloy on the Mo distribution throughout the grains and along grain boundaries (specimens aged 2 h at 700 °C). (**a**) Bright-field TEM image and corresponding diffraction pattern in <001> orientation. (**b**) Corresponding dark-field image formed with the 1/5>420< reflection indicated by the arrow in (**a**) showing domains of Ni$_4$Mo. (**c**) X-ray spectrum derived from the Ni$_4$Mo domain marked 1 in (**b**). (**d**) X-ray spectrum derived from the matrix region marked 2 in (**b**). (**e**) Auger spectrograph showing the Mo concentration as a function of distance from grain boundary
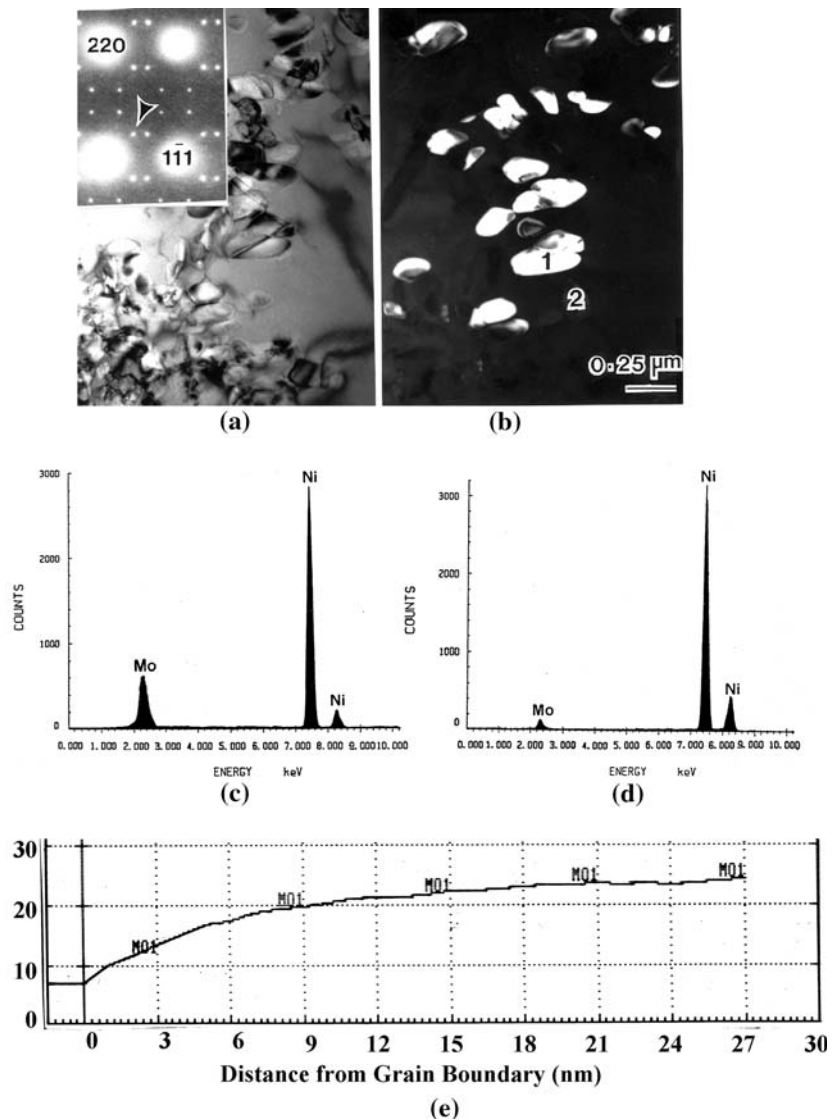
on the corrosion rate of the Ni–27Mo alloy. It is observed that a considerable increase in corrosion rate occurred after aging at 600–800 °C reaching a maximum value at 700 °C. Corresponding to this behavior was a considerable loss of tensile ductility, which could be related to the rapid kinetics of long-range ordering to Ni_4Mo at 700 °C. Corrosion in the annealed condition was primarily of the uniform or general type as shown in the example of Fig. 1b. However, after aging for 2 h at 700 °C, significant intergranular attack was observed as shown in Fig. 1c.

Analytical electron microscopy and Auger spectroscopy indicated that the above observations could be related to the redistribution of Mo throughout the grains and near grain boundaries as summarized in Fig. 2. Domains of Ni_4Mo in >001< orientation are shown in the bright-field image and corresponding diffraction pattern of Fig. 2a. Characteristic D1a superlattice reflections of Ni_4Mo are observed at 1/5 >420< positions. A dark-field image formed with the arrowed superlattice reflection in Fig. 2a is shown in Fig. 2b. Microchemical analysis revealed considerable Mo depletion of the matrix phase in the vicinity of Ni_4Mo domains as illustrated in the energy dispersive X-ray spectra of Fig. 2c and d. It is possible that this behavior could be due to the difficulty to reestablish equilibrium composition near the Ni_4Mo-matrix interface because of the slow diffusivity of Mo. Molybdenum-depleted zones were also observed alongside grain boundaries as demonstrated in the Auger spectrograph of Fig. 2e, which was generated by in-situ fracture of a specimen aged for 2 h at 700 °C followed by sputtering at a rate of 1 nm/min.

Comparative corrosion rates of the Ni–27Mo alloy and the Ni–27Mo–Cr alloys included in the study after 2 h of aging at 500–900 °C are shown in Fig. 3. As can be seen, both the Ni–27Mo–2Cr and Ni–27Mo–3Cr
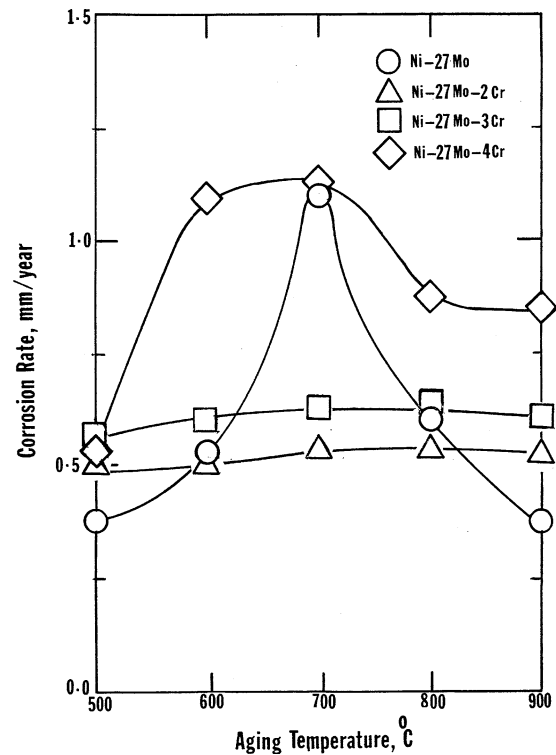
Fig. 3 Effect of 2 h of aging at various temperatures on the corrosion rate of Ni–Mo and Ni–Mo–Cr alloys in boiling 20% HCl

alloys maintained a corrosion rate comparable to that in the annealed condition of the Ni–2Mo alloy. A similar behavior was observed in the case of tensile ductility. In contrast, a considerable increase in corrosion rate was observed in the case of the Ni–27Mo–4Cr alloy reaching a peak value at 700 °C similar to the case of the Ni–27Mo alloy. These observations could be interpreted in terms of the effect of Cr addition on the ordering behavior as explained below.
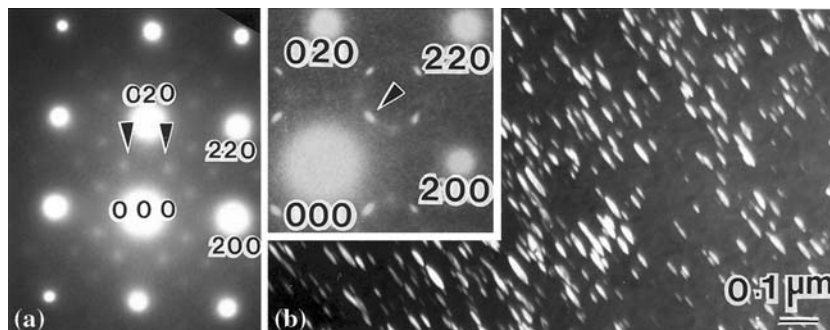
Fig. 4 Comparative structural features of the Ni–Mo–Cr alloys after 2 h of aging at 700 °C. (a) <001> diffraction pattern representative of the Ni–27Mo–2Cr and Ni–27Mo–3Cr alloys illustrating the presence of short-range order as indicated by the arrows. (b) <001> diffraction pattern and corresponding dark-field image formed with the 1/3<220> reflection marked by the arrow illustrating ordered domains of a Pt_2Mo-type superlattice in the Ni–27Mo–4Cr alloy

After up to 2 h of aging at 500–900 °C, only short-range order was observed in the Ni–27Mo–2Cr and Ni–27Mo–3Cr alloys similar to the annealed condition as shown in <001> diffraction pattern of Fig. 4a containing diffuse short-range order reflections at {1 1/2 0} positions. However, the Ni–27Mo–4Cr alloy was found to be ordered to a Pt_2Mo-type superlattice isomorphous with Ni_2Cr as indicated by the characteristic superlattice reflections at 1/3 <420> positions or equivalently at 1/3 <220> positions in Fig. 4b. It is to be noted that a Pt_2Mo-type superlattice of Ni_2Mo is not thermodynamically stable in the binary Ni–Mo system, however, it could be stabilized by additions of Cr with a composition of the type $Ni_2(Cr,Mo)$. Characteristic domains of this phase are shown in the dark-field image of Fig. 4b.

In conclusion, it was shown that critical additions of Cr to a Ni–27Mo alloy could be effective in decelerating the kinetics of long-range ordering to Ni_4Mo, which was found to have detrimental effects on corrosion resistance as well as mechanical strength. In the meantime, the Cr-containing alloys maintained a corrosion resistance comparable to that of the Cr-free alloy. More details about the ordering mechanism in these alloys will be published later.

References

1. Svistunova TV (2005) Met Sci Heat Treat 47(7/8):383
2. Friend WZ (1980) Corrosion of nickel and nickel-base alloys. John Wiley and Sons, New York, p 248
3. Uhlig HH (1971) Corrosion and corrosion control, 2nd edn. John Wiley and Sons, New York, p 355
4. Galen F Hodge (1983) In: Schweitzer PA (ed) Corrosion and corrosion protection handbook. Marcel Dekker, New York, p 55
5. Tawancy HM (1995) Mater Sci 30:522
6. Tawancy HM, Abbas NM (1988) J Mater Sci 24:1845
7. Tawancy HM (1984) Scripta Met 18:343